Journal of Molecular Liquids 402 (2024) 124759

Contents lists available at ScienceDirect

Journal of Molecular Liquids

journal homepage: www.elsevier.com/locate/molliq

Effect of cationic lipid concentration on monomer transfer kinetics between zwitterionic lipid vesicles

L. Bar [a], M.E. Villanueva [a], A. Sánchez-Rodríguez [a], J. Goole [b], P. Grosfils [c], P. Losada-Pérez [a,*]

[a] Experimental Soft Matter and Thermal Physics (EST) group, Department of Physics, Université Libre de Bruxelles, Boulevard du Triomphe CP 223, 1050 Brussels, Belgium
[b] Laboratory of Pharmaceutics and Biopharmaceutics, Université libre de Bruxelles, Campus la Plaine, CP 207, Boulevard du Triomphe, Brussels 1050, Belgium
[c] Center for Nonlinear Phenomena and Complex Systems, Department of Physics, Université Libre de Bruxelles, Boulevard du Triomphe CP223, 1050 Brussels, Belgium

ARTICLE INFO

Keywords:
Phase transitions
Non-equilibrium states
Lipid transfer
Cationic lipids
Quartz crystal microbalance with dissipation

ABSTRACT

The kinetics of spontaneous monomer transfer between vesicles consisting of zwitterionic phospholipids is dictated by the difference in desorption rate of lipid monomers from their donor vesicles and the concentration imbalance in the dispersion. In a system with two lipid species with the same headgroup, transfer is asymmetric, and takes place from the population of donor vesicles consisting of shorter chain lipids to acceptor ones of longer chain. Transfer typically proceeds until equilibrium is reached, resulting in populations of vesicles consisting of a binary mixture of both lipid species, whose concentration depends on the number of lipids in the precursor donor and acceptor vesicles before transfer.

Upon the introduction of a second lipid species in the donor vesicle population, the desorption rate of monomers should change with time, since the composition of donor vesicles changes when monomers of a given lipid type desorb. To tackle this problem, we added a cationic lipid, 1,2-dimyristoyl-3-trimethylammonium-propane (DMTAP), into donor zwitterionic lipid vesicles and assessed how the concentration of DMTAP affects the lipid transfer process. Lipid transfer is the result of the interplay between the initial concentration of DMTAP in the donor vesicles (and related probability of desorption at short transfer times) and their concomitant time-dependent concentration (and thus desorption rate) change due to the depletion of monomer species as the transfer process proceeds.

1. Introduction

The transfer of lipid molecules among liposomes can take place via several mechanisms like fusion and lipid monomer transfer [1,2]. The former is a multi-step process aided by proteins, ubiquitous in biology and involved in many events, such as viral infection and neurotransmitter release [3,4]. Protein-free lipid transfer can take place via different mechanisms like hemifusion between oppositely charged membranes (vesicles and planar bilayers) [5] or monomer transfer by diffusion in the aqueous media, the latter having been observed in processes involving lipid metabolism [6]. Monomer transfer between lipid vesicles takes place by diffusion through the aqueous medium. At low lipid concentrations, lipids are desorbed from the donor vesicle, diffuse through the aqueous medium and are finally absorbed by the acceptor vesicle [2]. The rate-limiting steps for the transfer process are the molecular desorption from the donor vesicle (with rate k^-) and the insertion into the host vesicle (with rate k^+). The energy barriers of both steps are dictated by the lipid's local hydrophobic environment and the membrane's interfacial structure and chemistry [7]. These depend on the lipid molecular features, namely, lipid hydrophobic chains (length and degree of saturation) and head group (size charge and orientation). The rate constants depend as well on the bilayer phase, being much faster in the liquid disordered phase than in the gel phase [8].

The kinetics of monomer transfer is typically described by deterministic models assuming that the absorption rate is proportional to the product of monomer numbers and the size of the lipid vesicle, while the desorption rate is proportional to the number of lipid molecules in the donor vesicle [9,10]. Lipid transfer entails time-dependent changes in composition and size of the vesicles in the system. As a matter of fact, monomers are very short-lived species with vanishing number most of the time. In the light of this, a stochastic version, termed direct transfer model of lipid transfer was recently introduced, where transfer can then

* Corresponding author.
E-mail address: patricia.maria.losada.perez@ulb.be (P. Losada-Pérez).

https://doi.org/10.1016/j.molliq.2024.124759
Received 16 January 2024; Received in revised form 31 March 2024; Accepted 14 April 2024
Available online 16 April 2024

be described in terms of direct exchange between vesicles without transiting via the monomer state [11]. In the direct transfer model, the vesicle size is defined by the number of lipids the vesicle contains. For a system with only one lipid species, the time dependence of the size distribution is purely diffusive (in the size space) and the average size of the vesicle does not change with time. For systems consisting of two lipid species the size distribution of the liposome dispersion is not only governed by diffusion, but also by the coupling between the concentration imbalance in the dispersion and the difference in desorption rates of both lipids from their donor vesicles [11]. For the particular case of zwitterionic lipids with the same headgroup but differing in their acyl chain length, spontaneous lipid transfer between vesicles is very asymmetric and takes place unidirectionally. Upon mixing the two (pure lipid) vesicle populations, the systems evolve from a non-equilibrium state at short times to equilibrium at longer times. The shorter chain lipid is desorbed faster than the longer chain one, thus the acceptor (longer chain length) lipid vesicles exhibit a time-dependent increase of their average size at the expense of the size decrease of (shorter) donor lipid vesicles, which get depleted of their lipid molecules [10]. The resulting equilibrium system consists of (on average) larger vesicles whose bilayer is a (equilibrium) binary mixture bearing the composition corresponding to the original number of lipids before mixing [10,11].

Understanding asymmetric lipid transfer is especially relevant in the context of protocell formation, where prebiotic vesicles have shown to be able to take lipids from each other [12,13]. In this regard, increasing the number of lipid species in donor and acceptor vesicles (before the transfer process starts) would be particularly interesting, since the system would likely evolve to a more complex scenario. From an experimental point of view, lipid transfer studies are typically restricted to nano-sized lipid vesicles of zwitterionic lipids with different chain length [8,10,14,15]. Lipid transfer experiments including diffusion of charged monomers are scarce and the few studies reported so far, have focused on the modification of the electrostatic surface potential of acceptor zwitterionic lipid vesicles from donor vesicles containing a small concentration of anionic lipid species [16]. This transfer follows a first-order kinetics with differences in the transfer rates for lipids with the same hydrophobic chain length but different headgroup. However, a direct relationship between transfer kinetics and headgroup features is not straightforward.

Lipid transfer involving cationic lipids is much less studied so far. At equilibrium, the impact of cationic lipids into zwitterionic lipid bilayers manifests at different levels: charged lipids are known to alter the physico-chemical properties of zwitterionic lipid bilayers mediated by electrostatic interactions between the head groups [17], and to modulate phase separation in multicomponent membranes [18]. From an application point of view, cationic lipids have been developed and intensively studied because of their application as carriers of DNA for transfection and nucleic acid delivery [19,20]. Vesicles consisting of unsaturated cationic lipids which display a conical shape like DOTAP tend to fuse, while the fusion efficiency decreases for saturated lipids which display a cylindrical shape like 1,2-dimyristoyl-3-trimethylammonium-propane (DMTAP) [21].

In this work we assess how the addition of cationic DMTAP lipids in donor zwitterionic vesicles impacts asymmetric lipid transfer with longer chain acceptor vesicles. The concentration of DMTAP is varied with a view to evaluate, on the one hand, how the presence of this lipid modifies monomer transfer directionality and, on the other hand, the possibility of fusion involved in the lipid transfer process. To this end, we make use of the equilibrium phase behavior of cationic-zwitterionic mixtures obtained by employing two complementary techniques, densitometry, and quartz crystal microbalance with dissipation monitoring (QCM-D). The connection between equilibrium phase behavior and non-equilibrium transfer is carried out in the following way. Donor and acceptor lipid vesicles are placed in contact under non-equilibrium conditions, lipid transfer is let to proceed in bulk at different fixed times (1 h, 3 h, 6 h, 12 h, 18 h, 24 h, 48 h and 72 h) and the phase behavior of the resulting vesicle populations after transfer at each time is analyzed by QCM-D.

2. Materials and methods

2.1. Materials

1,2-dimyristoyl-*sn*-glycero-3-phosphocholine (DMPC – in powder form), 1,2-dipalmitoyl-*sn*-glycero-3-phosphocholine (DPPC – in powder form) and DMTAP (dissolved in chloroform) lipids were purchased from Avanti Polar Lipids (Alabaster, AL) and spectroscopic grade chloroform from Analar (Normapur). HEPES buffer (pH 7.4) consisting of 10 mM HEPES (99 %) and 150 mM NaCl (≥99.5 %), both from Sigma-Aldrich was utilized for the hydration of the dried lipid films.

2.2. Vesicle preparation

The quantities of lipids were determined gravimetrically using an analytical balance (AG245, Metter-Toledo, Switzerland) with a precision of ± 0.1 mg. For equilibrium measurements, the pure lipids, as well as the lipid mixtures were first dissolved in chloroform; the solvent was then evaporated under a mild flow of nitrogen in a round-bottomed flask. The resulting lipid films were kept under vacuum overnight to remove any residual solvent. The films were then hydrated with HEPES buffer to 2 mg/ml under continuous stirring in a temperature-controlled water bath at a $T = 60$ °C (well above the melting temperature of all lipids) leading to multilamellar vesicles (MLVs). Large unilamellar vesicles (LUVs) were formed by extrusion through filters of 100 nm pore size for 25 passes in order to obtain vesicle dispersions with well-defined sizes. The extruded vesicle dispersions consisting of pure or mixed lipids at different mole fractions were diluted at 0.5 mg/ml. For the study of binary or ternary mixtures, these solutions were directly used.

For lipid transfer experiments, extruded vesicles consisting of selected DMPC:DMTAP mixtures at fixed (molar) ratio, namely 50:50, 80:20 and 20:80, and pure DPPC were diluted at the same molar ratio before being mixed at equivalent volumes (the final molar concentrations being all at 0.25 mM, corresponding to mass concentrations in the range of 0.34–0.35 mg/ml). Lipid transfer was carried out at $T = 60$ °C (all lipids in liquid disordered phase) in a temperature-controlled incubator (Incu-Line 68R, VWR, Poland; temperature stability ± 0.1 °C).

2.3. Dynamic light scattering (DLS)

Vesicle diameters and polydispersity indexes were determined by DLS (Malvern Zetasizer Nano ZS, Malvern, UK). For these measurements LUV dispersions in HEPES buffer at a 0.1 mg/ml concentration were used. The number of performed measurements per sample was at least $n = 4$ and measurements were carried out at room temperature. Zeta potential of all types of vesicle dispersions were determined by electrophoretic measurements using disposable folded capillary cells (Malvern, UK) placed in the same instrument.

2.4. Quartz crystal microbalance with dissipation monitoring (QCM-D)

A Qsense E4 instrument (Gothenburg, Sweden) monitoring the frequency and dissipation changes, $\Delta f/n$ and ΔD (for overtones n going from 3 to 13) has been used. Q-sense E4 also enables heating or cooling temperature scans in the range between $T = 15$ °C and $T = 65$ °C. AT-cut quartz crystals with Au coating (diameter 14 mm, thickness 0.3 mm, quoted surface roughness < 3 nm, and resonant frequency 4.95 MHz) were used. The Au-coated quartz sensors were UV-ozone treated with a UV-ozone cleaner (Bioforce Nanosciences, Germany) for 15 min, cleaned for 5 min with a 5:1:1 mixture of Milli-Q water (resistivity of 18.2 MΩ cm at $T = 25$ °C), ammonia and hydrogen peroxide heated at $T = 75$ °C, rinsed in Milli-Q water and dried with N_2. The lipid vesicles were injected into the QCM-D cells with a flow rate of 50 μl/min. Vesicle

adsorption onto the Au-coated sensors was carried out at $T = 15$ °C.

The experiments consisted in the following sequence: first, a baseline with pure HEPES buffer was established and afterwards lipid vesicles were injected over the Au-coated sensor chips. After reaching a stable intact supported vesicle layer, the pump was switched off and the ensemble was left to stabilize for 30 min. Subsequent heating and cooling temperature scans between $T = 15$ °C and $T = 60$ °C were performed at a rate of 0.4 °C/min, maintaining a 60 min stabilization time between successive temperature ramps.

2.5. Contact angle measurements

Contact angle (CA) measurements were carried out using an Attension ThetaLite instrument from Biolin Scientific (Sweden) based on the sessile drop method. A small drop (3 μl) of Milli-Q water was dispensed onto clean, UV-ozone treated Au-coated quartz surface, and the shape of the drop formed on the surface was analysed. Measurements were carried out at room temperature for 10 s using a recording speed of 20 frames/s. The average of all contact angles measured for the Au-coated quartz surfaces was estimated to be 29 ± 5°.

2.6. Density measurements

Density measurements were carried out using a DMA5000 densimeter from Anton Paar within a temperature range of $T = 15$ to $T = 60$ °C with steps of 0.3 °C between consecutive measurements. From the obtained density values, the specific volume v_s was calculated via [22]:

$$v_s = \frac{1}{c}\left(\frac{1}{\rho_d} - \frac{1-c}{\rho_s}\right) \quad (1)$$

where ρ_d and ρ_s are the density of the dispersion and HEPES buffer, respectively, and c is the weight fraction of the lipids in the dispersions. MLVs were used for density measurements at a concentration of 3 mg/ml.

3. Results and discussion

The time-dependent inter-bilayer lipid transfer taking place among two vesicle populations containing zwitterionic and cationic lipids was monitored by following the changes in the main phase transition as the transfer process takes place. In order to help deciphering the concentration changes with time as a result of monomer transfer, binary and ternary mixture phase diagrams of the lipids under study were determined at equilibrium, using density and QCM-D measurements. The former provides information about the changes in specific volume (and thus changes in lipid packing in the mixture) and it is used as a bulk, state-of-the-art, technique to validate the phase diagrams obtained by QCM-D. In fact, densitometry makes use of polydisperse multilamellar vesicles at a high concentration, while QCM-D uses LUVs dispersions with well-defined size and small concentration, thus being more appropriate for lipid transfer studies, where stable size vesicle dispersions are required.

3.1. Cationic and zwitterionic lipid mixtures at equilibrium

For all the studied cases, the main phase transition temperatures T_m were from the transition temperature derivatives of the specific volume obtained by density measurements and from the temperature derivative frequency and dissipation shifts obtained from QCM-D measurements [23–27]. It is worth mentioning that both frequency and dissipation temperature first-order derivatives provide similar phase transition temperature ranges [28]. Thus, both parameters will be used indistinguishably throughout this work. Fig. 1 shows as example the phase transition behavior of pure DMPC and DPPC vesicles. Panel A displays the specific volume of pure DMPC and pure DPPC MLVs, characterized by a discontinuity at the transition, as well as extrema in the first-order temperature derivative (panel B). Panels C and D show the frequency shifts and their respective first-order derivatives, obtained by QCM-D upon heating LUVs of DMPC and DPPC. As it can be observed, the transitions are very clear both in bulk (panel B) and when vesicles are solid-supported (panel D) and show quite a good agreement in the temperature range over which they take place.

Fig. 2 provides an overview of the main transition peaks of DMPC:

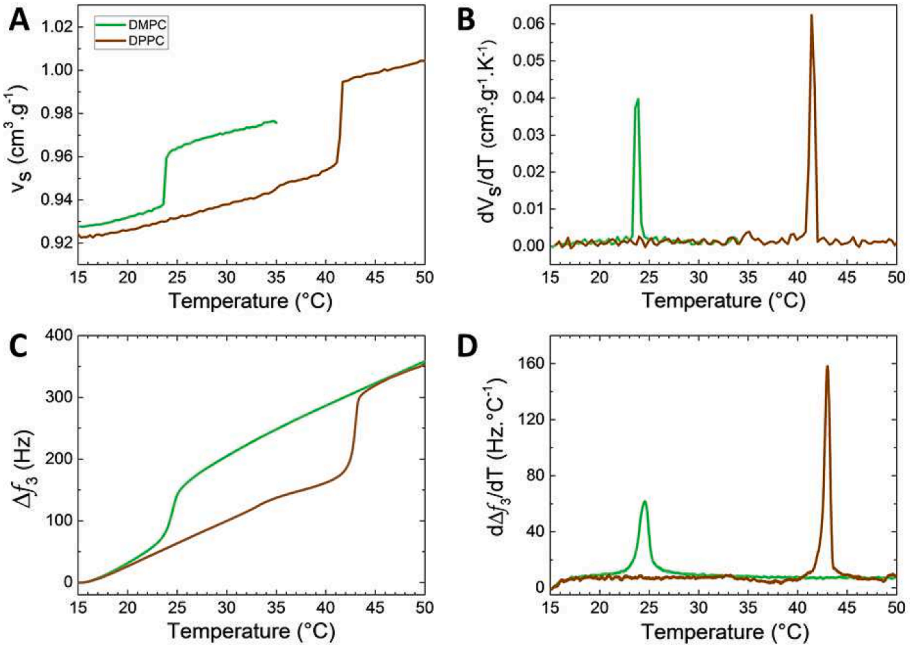

Fig. 1. Temperature dependence of the specific volume (panel A) and its first-order temperature derivative (panel B) for DMPC (green curves) and DPPC (brown curves) MLVs. Temperature dependence of the frequency shift (panel C) and the its first-order temperature derivative (panel D) for DMPC and DPPC LUVs adsorbed onto Au-coated QCM-D sensors. (For interpretation of the references to colour in this figure legend, the reader is referred to the web version of this article.)

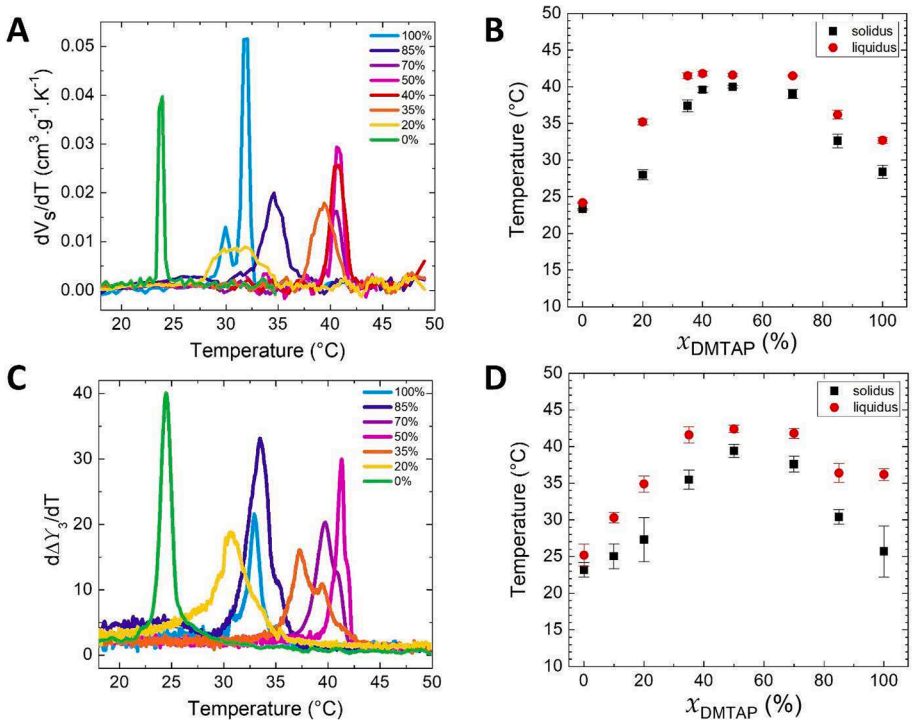

Fig. 2. Temperature dependence of first-order derivative of the specific volume (panel A) for MLVs consisting of binary mixtures of DMPC and DMTAP at different DMTAP mole fraction (in %). The corresponding phase diagram is displayed in Panel B. Temperature dependence of the first-order temperature derivative of ΔY, where Y stands for frequency or dissipation changes at the third overtone, (panel C) for LUVs consisting of binary mixtures of DMPC and DMTAP at different mole fractions (in %). The corresponding phase diagram is displayed in Panel D.

DMTAP mixtures, obtained from the temperature-dependent derivatives of the specific volume and of the frequency or dissipation shifts, respectively. The corresponding phase diagrams (panels B and D) were mapped by locating the onset and offset of the transition peaks. The addition of cationic DMTAP phospholipid into zwitterionic bilayers leads to a non-monotonic shift of the main phase transition temperature

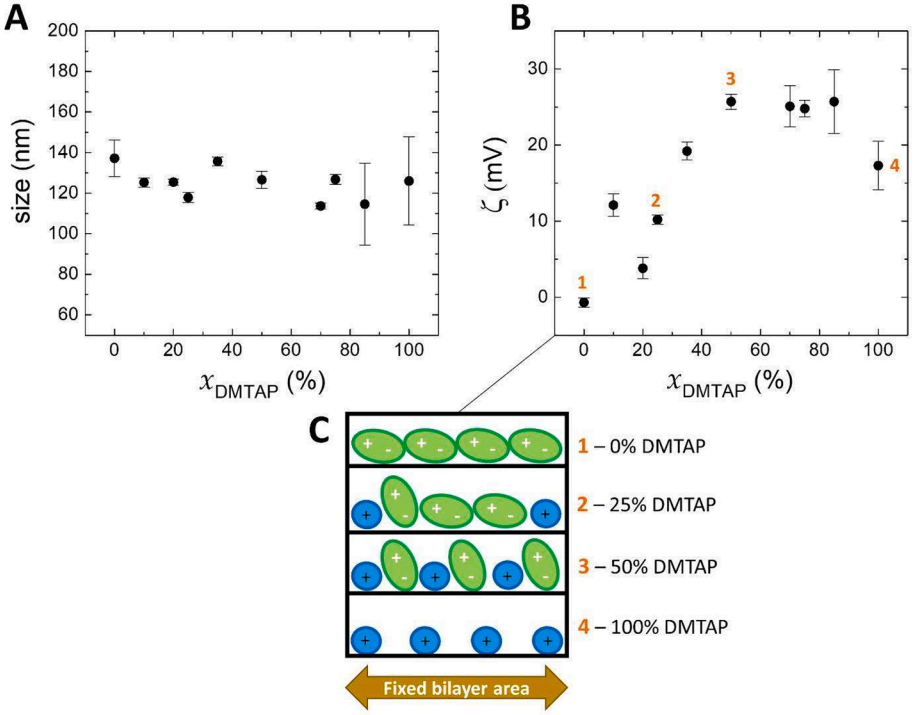

Fig. 3. Z-average size (panel A) and zeta potential (panel B) vs DMTAP percentage for vesicles consisting of DMPC:DMTAP mixtures. Panel C shows a scheme of how the headgroup charge orientation (PC green, TAP blue) impacts the area per molecule depending on the mole fraction percentage of DMTAP [17]. Experiments were performed at T = 25 °C in triplicate, and reported data are averages of all results. (For interpretation of the references to colour in this figure legend, the reader is referred to the web version of this article.)

with increasing DMTAP concentration. For DMPC-DMTAP mixtures with mole fraction $x_{DMTAP} < 0.5$, there is a continuous increase in T_m reaching a maximum between $x_{DMTAP} = 0.4$ and 0.5. These results agree qualitatively with previous calorimetric measurements performed in milli-Q water [29,30].

Likewise, molecular dynamics simulations have shown that the area per molecule in DMPC:DMTAP mixtures shows a minimum between $x_{DMTAP} = 0.4$ and 0.5 [17]. At small DMTAP mole fractions, the reorientation of PC headgroups driven by electrostatic interactions leads to the compression of the bilayer, since PC groups can pack more tightly with neighbouring TAP groups than in the case of PC alone. The optimal packing mole fraction is very close to equimolarity, since DMPC and DMTAP have the same number of carbons in their hydrophobic tails. The volume per molecule obtained from density measurements shows indeed a minimum (see Fig. S1 in the Supplementary Material). Close to the equimolar mixture, the volume and area per molecule are reduced by ~ 12.5 % (in relative terms) with respect to pure DMPC. DPPC:DMTAP mixtures follow the same pattern of behavior as a result of the electrostatic attraction between the PC and TAP groups. Yet, the main transition shift towards higher temperatures (at mole fractions $x_{DMTAP} < 0.5$) is smaller than for DMPC:DMTAP mixtures, since the packing of hydrophobic tails is less effective − due to the difference in acyl chain length between DPPC and DMTAP− (see Fig. S1 in the Supplementary Material). The volume per molecule is reduced by ~ 6 % (in relative terms) at the equimolar mixture with respect to pure DPPC. The phase diagram of DPPC:DMTAP mixtures obtained from QCM-D measurements can be found in Fig. S2 of the Supplementary Material.

Fig. 3 shows concentration-dependent hydrodynamic diameter (Z-average values) and zeta potential values of the DMPC:DMTAP mixtures at equilibrium, obtained from DLS and electrophoretic measurements. The average hydrodynamic radius of freshly extruded lipid vesicles remains quite constant with DMTAP concentration (panel A), whereas the size of pure DMTAP vesicles increases with time (see Fig. S3 in the Supplementary Material). As a matter of fact, phospholipids with TAP headgroup have shown a tendency to aggregate with increasing concentration of NaCl [31,32]. As regards the zeta potential, it shows a maximum around the equimolar concentration due to the surface charges exposed to the medium, consistent with the decrease in area and volume per molecule (see panel C of Fig. 3). Equivalent results for DPPC:DMTAP mixtures follow a similar trend (the maximum is less pronounced) and can be found in Fig. S4 of the Supplementary Material.

Phase transition coordinates will be used in the next section as the kinetic descriptor during lipid transfer experiments, for which stable vesicle dispersions with a well-defined size and phase transition peak are required. The above-exposed results show that lipid vesicles consisting of DMPC and DMTAP mixtures display quite a well-defined size and main phase transition peak (except for large DMTAP concentrations). In order to evaluate the effect of cationic lipids on the lipid transfer process, we have chosen three molar concentrations of DMPC:DMTAP mixtures, namely 80:20, 50:50 and 20:80, as vesicle populations to be mixed with a vesicle dispersion of pure DPPC. In Figure S5 of the supplementary information, we show the examples of pure DPPC and DMPC:DMTAP 50:50 to show the time-dependent stability of the phase behavior of vesicle populations used for the transfer experiments.

3.2. Lipid transfer experiments

We have chosen to use 100 nm-diameter LUVs for lipid transfer, for which curvature effects are not as important as for small unilamellar vesicles (SUVs). For the latter, curvature induces bending of the outer leaflet, leading to its expansion, whereas the inner leaflet gets compressed thus affecting the lipid transfer kinetics [33].

As mentioned in section 2.2, lipid transfer was carried out at $T = 60$ °C in a temperature-controlled incubator. At given times, i.e., 1 h, 3 h, 6 h, 12 h, 18 h, 24 h, 48 h, 72 h, after transfer has started, transfer was stopped by cooling the samples at 16 °C (gel phase). In this phase, transfer by monomer diffusion is dramatically reduced [15], thus one can assume that lipid transfer has stopped before injecting the samples in the QCM-D modules or their size measurement by DLS. Fig. 4 displays an overview of the phase transition signatures and the size distribution functions during the transfer process between LUVs of pure DPPC and DMPC:DMTAP mixtures. After incubation at T = 60 °C, their phase transition behavior and size distribution were measured by QCM-D and DLS at fixed times after the beginning of the transfer process. For the sake of clarity, we will discuss the transfer between DPPC LUVs and LUVs of each DMPC:DMTAP mixture separately.

3.2.1. Transfer between DPPC and DMPC:DMTAP (80:20)

Before the beginning of the transfer process, the size distribution of both extruded vesicle populations was checked and is characterized by single peaks centered at around 100 nm diameter. Their main transitions are characterized by well-defined peaks displaying different transition temperatures (T_m ~ 33.3 °C for DMPC:DMTAP 80:20 and T_m ~ 42.5 °C for pure DPPC).

At short times after the transfer process starts ($t = 1$ h), the high-T peak (the peak originally corresponding to pure DPPC vesicles) is shifted towards lower temperatures, while the low-T peak is slightly shifted towards higher temperatures. This indicates that unidirectional transfer of DMPC monomers take place from DMPC-rich donor vesicles towards DPPC acceptor ones. DMPC donor vesicles get depleted of DMPC (the most abundant component in the donor LUVs), decreasing in size and changing composition (increasing concentration in DMTAP, thus increasing in phase transition temperature according to the phase diagram in Fig. 2D). In turn, DPPC acceptor vesicles absorb DMPC monomers, they increase in size, and their phase transition temperature decreases. The two transition peaks merge at intermediate times leading to a broad transition, while at longer times ($t \geq 18$ h), a single peak is observed, whose position and shape remains rather constant (T_m ~ 37.2 °C). The time-dependent size distributions obtained by DLS display the behavior predicted by a recently introduced direct transfer model involving two lipid species [10]. Specifically, at short times the distribution gets broadened and the peak maximum is slightly shifted towards lower sizes, while at longer times an additional mode appears (see Figure S6 in the Supplementary Information). For completeness, the size stability of pure DPPC and the DMPC:DMTAP (80:20) mixture when LUVs when incubated separately has been checked over time after extrusion (see Figure S7 in the Supplementary Information). While the DPPC size distribution remains stable, DMPC:DMTAP (80:20) vesicles display an additional population of very large hydrodynamic diameter (1270 ± 345 nm) after 72 h most likely due to vesicle fusion. A population of very large vesicles is however not observed after 72 h of lipid transfer experiment, indicating that fusion in the DMPC:DMTAP population is precluded by the transfer process of DMPC monomers towards DPPC acceptor vesicles (acceptor vesicles diminish in size at the expense of the donor vesicles).

In order to assess the impact of a rather small amount of DMTAP in the transfer process kinetics, it is instructive to compare it with the transfer between pure DMPC and DPPC vesicles populations in the absence of DMTAP, recently reported by our group [14]. Fig. 5A displays phase transition peaks before and after 48 h transfer between DPPC and DMPC in the absence and presence of 20 % mol DMTAP in DMPC donor vesicles. Fig. 5B shows a comparison of the time-dependent melting temperature decrease of acceptor DPPC vesicles when exposed to i) pure DMPC vesicles and ii) DMPC:DMTAP (80:20) of similar size. Pure DMPC vesicles provide more DMPC molecules (larger ΔT_m shifts) to be transferred to DPPC during the same time than similar size DMPC:DMTAP (80:20) ones. Considering that the monomer desorption rate is proportional to the concentration of molecules in the bilayer state [9], desorption of DMPC from pure DMPC vesicles should be faster than from DMPC:DMTAP (80:20). If we now assume DMPC desorption depends solely on molecular concentration (DMTAP molecules do not affect DMPC desorption), we would expect a kinetic profile as shown by the

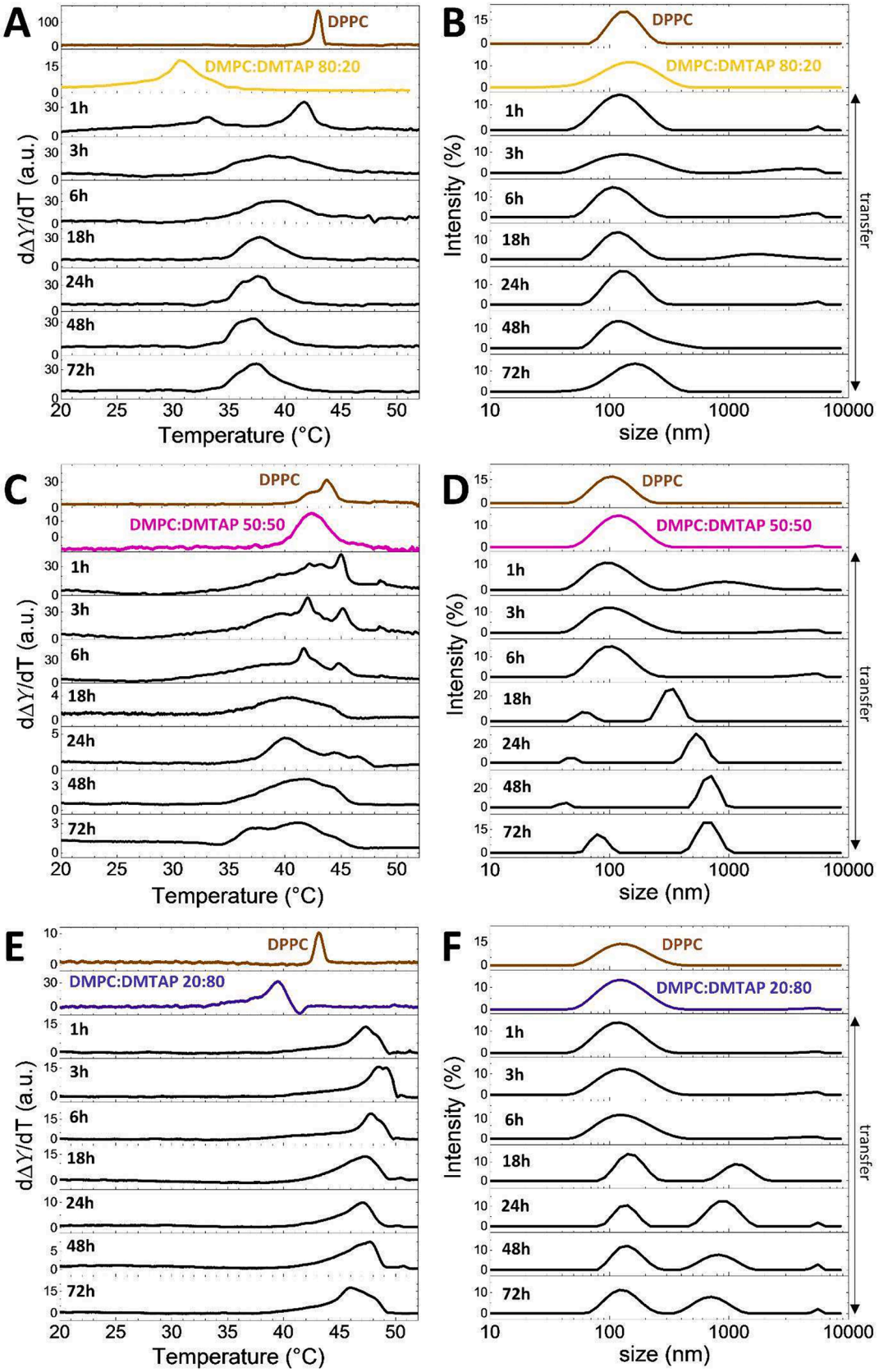

Fig. 4. Time-dependent main phase transition peaks (panels A, C, E) and size distributions (panels B, D, F) of LUV populations after the transfer process between DPPC and DMPC:DMTAP (80:20, 50:50 or 20:80) mixed at equimolarity. Names in colour refer to vesicle populations before the transfer process.

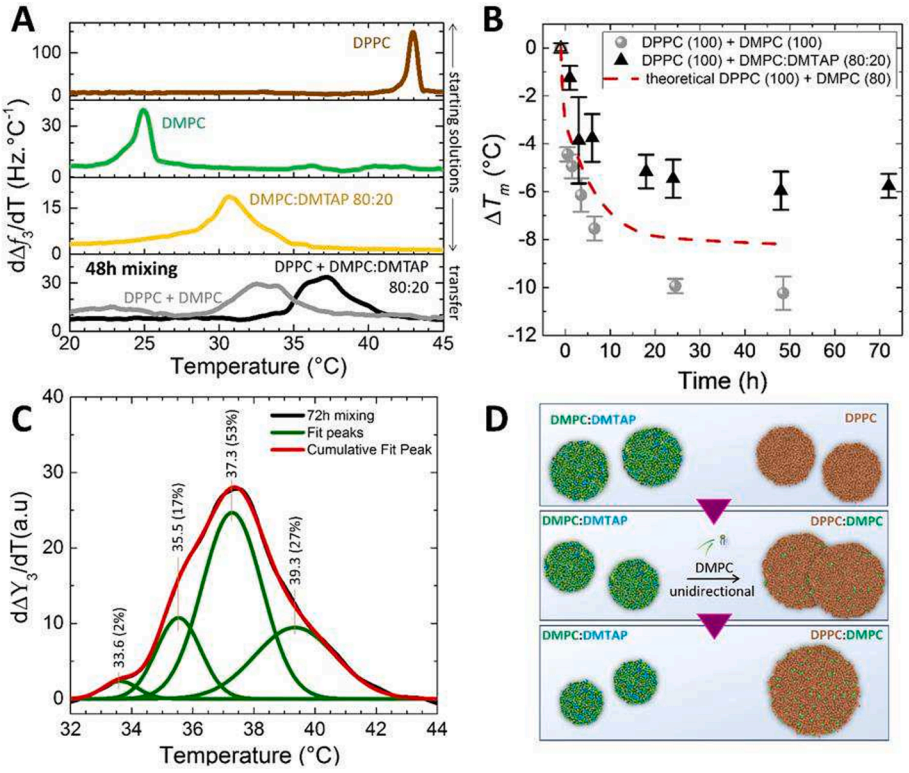

Fig. 5. Comparison of lipid transfer between DPPC and DMPC LUVs in presence and absence of DMTAP. Panel A: Main phase transition peaks vesicle populations before transfer and 48 h after the beginning of the transfer process. Panel B: Time-dependent ΔT_m values extracted from high-T peaks. Panel C: 72 h main transition peak deconvolution. Panel D: Schematic of the proposed transfer process.

dashed line. The dashed line was obtained considering that in DMPC:DMTAP LUVs there are 20 % less DMPC molecules than in pure DMPC LUVs (thus multiplying the pure DMPC transfer kinetic curve (grey symbols) by 0.8). Clearly, experimental results show that this is not the case, indeed electrostatic interactions between PC and TAP groups decrease the desorption rate of DMPC in the presence of cationic lipids. Although one cannot rule out the desorption and transfer of DMTAP, this is less prone to happen given the charge/concentration ratio in which it is present in these vesicles. Fig. 5C shows the peak deconvolution of the main transition peak after 72 h of lipid transfer. The intensity and the shape of the QCM-D peaks scale with the composition of the vesicles (one-component vesicles show typically narrower and more intense peaks), as well as with the thickness and number of the vesicles adsorbed [34]. The deconvolution of the peaks shows the coexistence of four vesicle populations. The most intense one is consistent with the presence of a large and most abundant vesicle population of DPPC:DMPC with composition close to 80:20 (see Figure S8B in the Supplementary Information). If one assumes that DPPC monomer desorption from acceptor vesicles is very unlikely, the remaining (less intense) peaks observed in panel C are consistent with a DMPC:DMTAP population with composition close to 70:30 (see the example of calculation in Supplementary information). In this respect, the underlying peaks agree with the unidirectional transfer picture provided by Fig. 5D.

3.2.2. Transfer between DPPC and equimolar mixture DMPC:DMTAP (50:50)

The transfer process between DPPC and a DMPC:DMTAP equimolar mixture shows a different pattern of behavior (see panels C and D of Fig. 4). The main transition temperature of both vesicle populations before transfer is very similar ($T \sim 42$ °C) since, at equimolarity, DMPC and DMTAP pack most efficiently driven by electrostatic attraction of their headgroups. One would expect that the transfer between these two vesicle populations is no longer unidirectional, since the desorption rate of the lipid species involved should be quite similar, given the similar melting temperatures displayed. However, taking into account the shorter length of DMPC and DMTAP and the fact that DPPC needs to disrupt the headgroup environment of PC and TAP groups to insert into these vesicles, it is more likely that transfer is dictated by either DMPC or DMTAP monomer desorption and insertion into DPPC. Panels C and D in Fig. 4 show that at short times after the transfer process began ($t \leq 6$ h), the phase transition of the system is characterized by very broad and complex peaks, covering a large temperature range below and above the transition of the two original vesicle populations. The fact that the peak is broadened towards lower and higher temperatures points that, at short times after the transfer begins, DMTAP is desorbed faster (its headgroup is smaller) than DMPC and inserts into acceptor DPPC vesicles. At $t \leq 6$ h, DLS measurements show a single size distribution where the average size tends to slightly decrease as compared to the average size of the original vesicle populations before transfer. As inferred from the phase diagram in Fig. 2D and shown in Figure S2 in the Supplementary Material, the addition of DMTAP at mole fractions below $x = 0.5$ induces an increase of T_m in DPPC acceptor vesicles, which leads to the appearance of a clear peak at $T \sim 45$ °C, visible at 1, 3, and 6 h after mixing. This peak is consistent with a DPPC:DMTAP (90:10) mixture of acceptor vesicles, according to the phase diagram in Fig. S2 panel B. Donor vesicles get depleted of DMTAP, their size decreases and their composition changes, becoming, in principle richer in DMPC. This entails a time-dependent change of monomer desorption rate from donor vesicles, which, after a given time, promotes desorption and transfer of DMPC as well. As a result, vesicle populations consisting of mixtures of DMPC:DMTAP and DPPC:DMTAP coexist after $t = 6$ h. At longer times ($t \geq 18$ h), the high-T peak observed at $T = 45$ °C merges with the shoulder at lower temperatures. As a matter of fact, at $t = 72$ h, the peak deconvolution is consistent with a most abundant population of equilibrium DPPC:DMPC:DMTAP 50:25:25 ternary mixture (see Fig. 6 and Fig. S8Ain the Supplementary Information), coexisting with a

population that would correspond to DMPC:DMTAP vesicles of composition around 70:30 (see Fig. 6B) and a less abundant population of DPPC:DMTAP mixture. Interestingly, at $t \geq 18$ h, DLS measurements show the coexistence of two vesicle populations, which at very long times are centered around dI = 79 ± 12 nm and dII = 660 ± 55 nm (see panel C), with I and II representing the two populations in size. Fig. 6D shows a schematic picture of the proposed time-dependent transfer process. As we shall see in the following section, the formation of the ternary mixture is probably aided by fusion.

3.2.3. Transfer between DPPC and DMPC:DMTAP (20:80)

The time-dependent phase transitions during transfer between DPPC ($T_m \sim 42.5$ °C) and DMPC:DMTAP ($T_m \sim 39.5$ °C) LUVs are displayed in panels E and F of Fig. 4. Overall, the main transition peaks get broadened and show a higher T_m than the ones displayed by initial vesicle populations before the transfer begins. Being most abundant, DMTAP monomers desorb from donor DMPC:DMTAP (20:80) vesicles and are transferred into acceptor DPPC, leading to higher transition temperatures. At the same time, the donor vesicle population decreases in size and its transition temperature shifts to smaller values. The compensation in the size decrease of donor and increase of acceptor vesicles is reflected in the fact that the size distribution obtained by DLS barely changes at short times. Fig. 7A and 7B show the peak deconvolution of the main transition peak at short ($t = 3$ h) and long times ($t = 72$ h) after the beginning of lipid transfer. At short times, the peak observed at $T = 48.8 \pm 0.7$ °C (deconvoluted into the two fit peaks at $T = 48.4$ °C and $T = 49.4$ °C in Fig. 7A) is consistent with a binary DPPC:DMTAP (65:35) mixture (see Fig. S2). The remaining peak is consistent with a DMPC:DMTAP (43:57) mixture, whose transition is expected to range from $T = 39$ °C and $T = 46$ °C (which, according to the phase diagram displayed in Fig. 2D). A similar approach as the one provided in the Supplementary Information to estimate vesicle composition after transfer has been used. With time, the phase transition peak shifts slightly and gets broadened towards lower temperatures. DLS measurements show a single population at short times ($t \leq 6$ h), whose maximum remains rather constant, resulting from a compensation in size changes between donor and acceptor vesicles. At this point, the desorption of both DMPC and DMTAP is possible, considering the fact that transfer between lipid vesicle populations is governed by the coupling between the concentration imbalance in the dispersion and the difference in desorption rates of lipids from their donor vesicles. The deconvolution of the $t = 72$ h peak is consistent with the coexistence of vesicle populations close to the compositions DPPC:DMTAP (80:20) and DMPC:DMTAP (27:73), indicating that DMTAP might have desorbed from DPPC:DMTAP population and transferred into DMPC:DMTAP one.

DLS measurements at long times ($t \geq 18$ h) show the coexistence of two size populations, d = 128 ± 16 nm and (d = 704 ± 80 nm), indicating that for vesicle populations containing DMTAP-phospholipid mixtures close to equimolarity, transfer at long times is not only driven by monomer diffusion but also by fusion. In fact, a detailed analysis of frequency shift plateaus by QCM-D upon adsorption of lipid vesicles at different times during the transfer process, shows that for systems where donor vesicles are DMPC:DMTAP mixtures with DMTAP concentration $x \geq 0.5$, a significant decrease in frequency shift takes place after long transfer times ($t \geq 18$ h) (see red circles and blue triangles in Fig. 8). In turn, for systems where donor vesicles are DMPC:

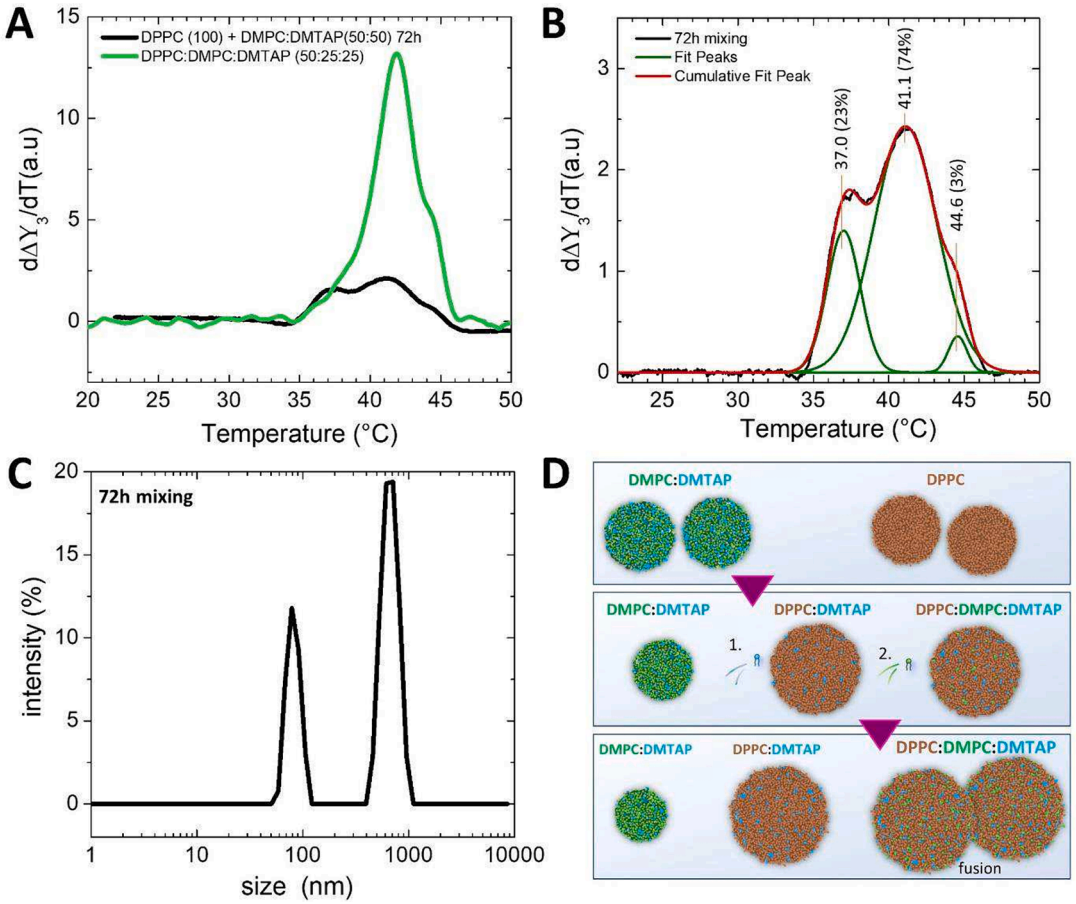

Fig. 6. Results arising from transfer between DPPC LUVs and DMPC:DMTAP 50:50 LUVs. Panel A: QCM-D phase transitions of the 72 h-sample with underlying experimental peak of ternary mixture. Panel B: 72 h main transition peak deconvolution. Panel C: Size distribution of the resulting populations obtained after 72 h. Panel D: Scheme of the proposed transfer process.

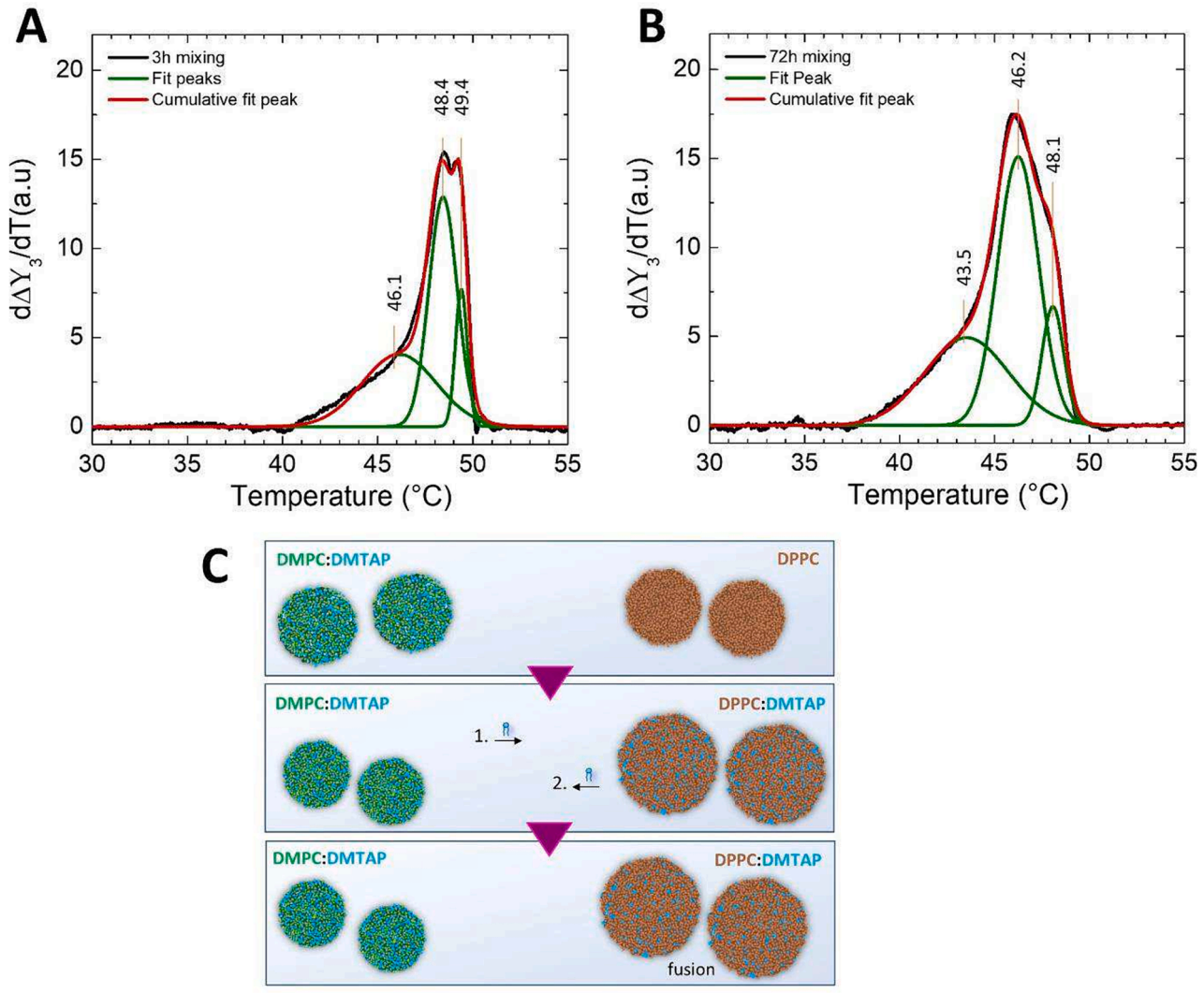

Fig. 7. Results arising from transfer between DPPC LUVs and DMPC:DMTAP 20:80 LUVs. Panel A: Deconvolution of the QCM-D peak obtained after 3 h mixing. Panel B: Deconvolution of the QCM-D peak obtained after 72 h mixing. The experimental peaks are in black whereas the cumulative fit peaks (in red) correspond to the sum of several fit peaks (in green). Panel C: Scheme of the proposed transfer process. (For interpretation of the references to colour in this figure legend, the reader is referred to the web version of this article.)

DMTAP mixtures with DMTAP concentration $x = 0.2$, the frequency shift remains rather constant with transfer time. The frequency shift decrease is compatible with the presence of very large vesicles of diameter larger than the deepest penetration depth of the evanescent acoustic wave in the vertical direction ($\delta \sim 250$ nm). The adsorption of systems with size ≥ 500 nm like cells leads to frequency shifts much smaller than 100 nm vesicles [35].

4. Conclusions

Lipid monomer transfer between vesicles composed of zwitterionic (DMPC and DPPC) lipids with different alkyl chain length has been studied upon the addition of a cationic lipid (DMTAP) in donor vesicles by assessing the time-dependent phase transition signatures using QCM-D. At equilibrium, DMTAP reduces the average molecular volume of zwitterionic lipids in a bilayer by electrostatic interactions between PC and TAP headgroups, leading to optimal packing close to equimolarity. This involves that, in PC:TAP mixtures, the desorption rate of lipid monomers is concentration-dependent, since it strongly depends on the number of hydrophobic contacts to be broken.

As a matter of fact, lipid transfer between donor DMPC vesicles containing DMTAP and acceptor DPPC vesicles has shown to be strongly dependent on the interplay between the initial composition of donor vesicles and time-dependent composition changes of both vesicle donor and acceptor vesicle populations. At low initial DMTAP concentration in donor vesicles, transfer is mainly asymmetric, with DMPC monomers desorbing from donor vesicles and being transferred to DPPC acceptor ones. The presence of a small fraction of DMTAP delays DMPC desorption as compared to pure DMPC, as a result of the increased packing (and slower desorption rate) between DMPC and DMTAP molecules in the donor bilayer.

At initial DMTAP concentrations ($x_{DMTAP} \geq 0.5$), transfer is governed by monomer desorption at short times, while vesicle fusion cannot be ruled out at longer times, as indicated by the vesicle size distributions obtained by DLS. Transfer between donor vesicles with DMPC:DMTAP equimolar concentration shows that DMTAP desorbs faster than DMPC, thus involving time-dependent concentration changes of both donor and acceptor vesicles, resulting in a most abundant vesicle population consisting of the three lipid species at equilibrium. At very large initial DMTAP concentrations, DMTAP being more abundant, desorbs very fast from donor vesicles and inserts into DPPC acceptor ones until two populations of DPPC:DMTAP and DMPC:DMTAP vesicles of concentrations close to equimolarity coexist, thus enabling bidirectional transfer due to the imbalance between concentrations in vesicle populations and

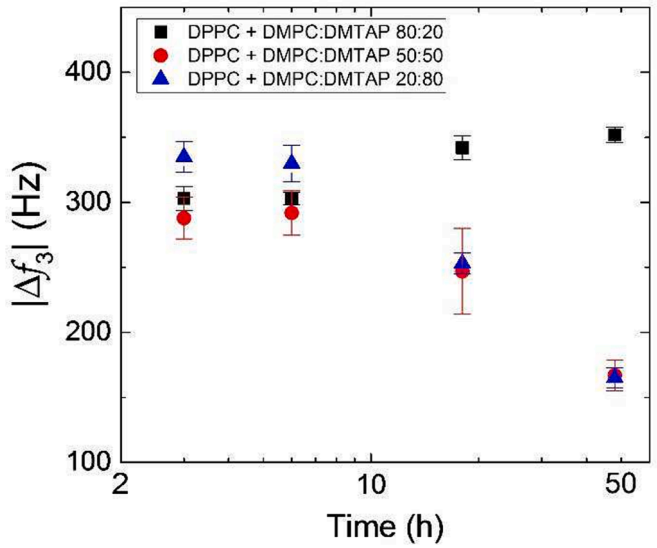

Fig. 8. QCM-D frequency shifts (in absolute value) observed for the adsorption of vesicles formed after several mixing times between DPPC and DMPC:DMTAP lipid vesicle dispersions.

desorption rates of lipids from donor vesicles. This results in two main DPPC:DMTAP and DMPC:DMTAP populations at equilibrium.

In summary, our results have shown that the interplay between initial lipid concentration in donor vesicles and the time-dependent changes in composition of both donor and acceptor vesicles govern lipid transfer kinetics and directionality. The experimental observations call for lipid transfer models that include the possibility of time-dependent change of desorption rates and which will be the subject of a follow-up investigation of this work.

CRediT authorship contribution statement

L. Bar: Writing – review & editing, Writing – original draft, Validation, Methodology, Formal analysis, Data curation. **M.E. Villanueva:** Writing – review & editing, Methodology, Formal analysis, Data curation. **A. Sánchez-Rodríguez:** Formal analysis, Data curation. **J. Goole:** Data curation, Conceptualization. **P. Grosfils:** Writing – review & editing, Supervision, Methodology, Conceptualization. **P. Losada-Pérez:** Writing – review & editing, Writing – original draft, Supervision, Methodology, Funding acquisition, Conceptualization.

Declaration of competing interest

The authors declare that they have no known competing financial interests or personal relationships that could have appeared to influence the work reported in this paper.

Data availability

Data will be made available on request.

Acknowledgements

P.L.P. acknowledges funding of the projects 'DELTA' project number 40008129 by the Fonds de la Recherche Scientifique (FNRS) 'SADI' n 20061 by the programme Action Recherche Concertée, Université Libre de Bruxelles (ULB).

Appendix A. Supplementary data

Supplementary data to this article can be found online at https://doi.org/10.1016/j.molliq.2024.124759.

References

[1] W. Wickner, R. Schekman, Membrane fusion, Nat. Struct. Mol. Biol. 15 (2008) 658.
[2] R.E. Brown, Spontaneous lipid transfer between organized lipid assemblies, Biochim. Biophys. Acta 1113 (1992) 375–389.
[3] R. Jahn, T. Lang, T.C. Südhof, Membrane Fusion 112 (2003) 519–533.
[4] S. Martens, H.T. McHanon, Mechanisms of membrane fusion: disparate players and common principles, Nat. Rev. Mol. Cell Biol. 9 (2008) 543–556.
[5] A. Kunze, S. Svedhem, B. Kasemo, Lipid transfer between charged supported lipid bilayers and oppositely charged vesicles, Langmuir 25 (2009) 5146–5158.
[6] O. Hernell, J.E. Staggers, M.C. Carey, Physical-chemical behavior of dietary and biliary lipids during intestinal digestion and absorption. 2. Phase behavior and aggregation states of luminal lipids during duodenal fat digestion in healthy adult human beings, Biochemistry 29 (1990) 2041–2056.
[7] J.L. Rogers, G. Espinoza-García, P.L. Geissler, Membrane hydrophobicity determines the activation free energy of passive lipid transport, Biophys. J. 120 (2021) 3718–3731.
[8] T.M. Bayerl, C.F. Schmidt, E. Sackmann, Kinetics of symmetric and asymmetric phospholipid transfer between small sonicated vesicles studied by high-sensitivity differential scanning calorimetry, NMR, electron microscopy and dynamic light scattering, Biochemistry 27 (1988) 6078–6085.
[9] L. Thilo, Kinetics of phospholipid exchange between bilayer membranes, Biochim. Biophys. Acta 469 (1977) 326–334.
[10] P. Grosfils, L. Bar, G. Cordoyiannis, P. Losada-Pérez, Interplay between size and concentration in unidirectional lipid transfer between zwitterionic vesicles under non-equilibrium conditions, J. Mol. Liq. 354 (2022) 118875.
[11] P. Grosfils, P. Losada-Pérez, Kinetic control of liposome size by direct lipid transfer, J. Colloid Int. Sci. 652 (2023) 1381–1393.
[12] Z. Cheng, P.L. Luisi, Coexistence and mutual competition of vesicles with different size distributions, J. Phys. Chem. B 107 (2003) 10940–10945.
[13] B. Shirt-Ediss, K. Ruiz-Mirazo, F. Mavelli, R.V. Solé, Modelling lipid competition dynamics in heterogeneous protocell populations, Sci. Rep. 4 (2014) 1.
[14] H.M. Reinl, T.M. Bayerl, Lipid transfer between small unilamellar vesicles and single bilayers on a solid-support: self-assembly of supported bilayers with asymmetric lipid distribution, Biochemistry 33 (1994) 14091–14099.
[15] L. Bar, G. Cordoyiannis, S. Neupane, J. Goole, P. Grosfils, P. Losada-Pérez, Asymmetric lipid transfer between zwitterionic vesicles by nanoviscosity measurements, Nanomaterials 11 (2021) 1087.
[16] J.L. Richens, A.I.I. Tyler, H.M.G. Barriga, J.P. Bramble, R.V. Law, N.J. Brooks, J. M. Seddon, O. Ces, P. O'Shea, Spontaneous charged lipid transfer between lipid vesicles, Sci. Rep. 7 (2017) 12606.
[17] A. Gurtovenko, M. Patra, M. Karttunen, I. Vattulainen, Cationic DMPC/DMTAP Lipid Bilayers: Molecular Dynamics Study, Biophys. J. 86 (2004) 3461–3472.
[18] Y. Wang, S. Majd, Charged lipids modulate the phase separation in multicomponent membranes, Langmuir 39 (2023) 11371–11378.
[19] J.B. Behr, Gene transfer with synthetic cationic amphiphiles: Prospects for gene therapy, Bioconjugate Chem. 5 (1994) 382.
[20] H.H.T. Zaks, R. Langer, Y. Dong, Lipid nanoparticles for m-RNA delivery, Nat. Rev. Mater. 6 (2021) 1078–1094.
[21] R. Kolašinac, C. Kleusch, T. Braun, R. Merkel, A. Csiszár, Deciphering the functional composition of fusogenic liposomes, Int. J. Mol. Sci. 19 (2018) 346.
[22] T.N. Murugova, P. Balgavý, Molecular volumes of DOPC and DOPS in mixed bilayers of multilamellar vesicles, Phys. Chem. Chem. Phys. 16 (2014) 18211.
[23] J.J.J. Gillissen, J.A. Jackman, S.R. Tabaei, N.J. Cho, A numerical study on the effect of particle surface coverage on the quartz crystal microbalance response, Anal. Chem. 90 (2018) 2238–2245.
[24] S.R. Tabaei, J.J.J. Gillissen, N.J. Cho, Probing membrane viscosity and interleaflet friction of supported lipid bilayers by tracking electrostatically adsorbed, nano-sized vesicles, Small 12 (2016) 6338–6344.
[25] S.R. Tabaei, J.J.J. Gillissen, S. Block, F. Höök, N.J. Cho, Hydrodynamic propulsion of liposomes electrostatically attracted to a lipid membrane reveals size-dependent conformational changes, ACS Nano 10 (2016) 8812–8820.
[26] S.R. Tabaei, J.J.J. Gillissen, S. Vafaei, J.T. Groves, N.J. Cho, Size-dependent stochastic nature of lipid exchange between nanovesicles and model membranes, Nanoscale 8 (2016) 13513–13520.
[27] M. Dacic, J.A. Jackman, S. Yorulmaz, V.P. Zhdanov, B. Kasemo, N.J. Cho, Influence of divalent cations on deformation and rupture of adsorbed lipid vesicles, Langmuir 32 (2016) 6486–6495.
[28] S. Neupane, Y. De Smet, F.U. Renner, P. Losada-Pérez, Quartz crystal microbalance with dissipation monitoring : A versatile tool to monitor phase transitions in biomimetic membranes, Front. Mater. 5 (2018) 46.
[29] R. Zantl, L. Baicu, F. Artzner, I. Sprenger, G. Rapp, J.O. Rädler, Thermotropic phase behavior of cationic lipid-DNA complexes compared to binary lipid mixtures, J. Phys. Chem. B 103 (1999) 10300–10310.
[30] S. Ahmed, S. Savarala, Y. Chen, G. Bothun, S.L. Wunder, Formation of lipid sheaths around nanoparticle-supported lipid bilayers, Small 8 (2012) 1740–1751.
[31] F. Bordi, C. Cametti, Salt-induced aggregation in cationic liposome aqueous suspensions resulting in multi-step self-assembling complexes, Colloids Surf. B Biointerfaces 26 (2002) 341–350.
[32] M. Ullrich, J. Haša, J. Hanuš, M. Šoóš, F. Štěpánek, Formation of multi-compartmental particles by controlled aggregation of liposomes, Powder Technol. 295 (2016) 115–212.

[33] T. Brumm, K. Jorgensen, O.G. Mouritsen, T.M. Bayerl, The effect of increasing membrane curvature on the phase transition and mixing behavior of a dimyristoy-sn-glycero-3-phosphatidylcholine/distearoyl-sn-glycero-3-phosphatidylcholine lipid mixture as studied by fourier transform infrared spectroscopy and differential scanning calorimetry, Biophys. J. 70 (1996) 1373–1379.

[34] N. Bibissidis, K. Betlem, G. Cordoyiannis, F. Prista-von Bonhorst, J. Goole, J. Raval, M. Daniel, W. Góźdź, A. Iglič, P. Losada-Pérez, Correlation between adhesion strength and phase behaviour in solid-supported lipid membranes, J. Mol. Liq. 320 (2020) 114492.

[35] D. Yongabi, S. Jooken, S. Givanoudi, M. Khorshid, O. Deschaume, C. Bartic, P. Losada-Pérez, M. Wübbenhorst, P. Wagner, Ionic strength controls long-term cell-surface interactions −A QCM-D study of S. cerevisiae adhesion, retention and detachment, J. Colloid Int. Sci. 585 (2021) 583–595.